Published in final edited form as:
J Biomed Mater Res A. 2010 June 1; 93(3): 1004–1015. doi:10.1002/jbm.a.32549.

In Vitro and In Vivo Platelet Targeting By Cyclic RGD-modified Liposomes

Rekha Srinivasan[1], **Roger E. Marchant**[1], and **Anirban Sen Gupta**[1,*]

[1] Case Western Reserve University, Department of Biomedical Engineering, 10900 Euclid Avenue, Cleveland, OH 44106

Abstract

Cell-selective delivery using ligand-decorated nanoparticles is a promising modality for treating cancer and vascular diseases. We are developing liposome nanoparticles surface-modified by RGD peptide ligands having targeting specificity to integrin GPIIb-IIIa. This integrin is upregulated and stimulated into a ligand-binding conformation on the surface activated platelets. Activated platelet adhesion and aggregation are primary events in atherosclerosois, thrombosis and restenosis. Hence platelet-targeted nanoparticles hold the promise of vascular site-selective delivery of drugs and imaging probes. Here, we report in vitro and ex vivo microscopy studies of platelet-targeting by liposomes surface-modified with a cyclic RGD peptide. The peptide-modified liposomes were labeled either with a lipophilic fluorophore or with lipid-tethered Nanogold®. For in vitro tests, coverslip-adhered activated human platelets were incubated with probe-labeled liposomes, followed by analysis with fluorescence and phase contrast microscopy, and scanning electron microscopy (SEM). For in vivo tests, the liposomes were introduced within a catheter-injured carotid artery restenosis model in rats and post-euthanasia, the artery was imaged ex vivo by fluorescence microscopy and SEM. All microscopy results showed successful platelet-targeting by the peptide-modified liposomes. The in vitro SEM results also enabled visualization of nanoscopic liposomes attached to activated platelets. The results validate our nanoparticle design for site-selective vascular delivery.

Keywords

platelets; targeting; drug delivery; cyclic RGD

1. Introduction

Platelet activation, adhesion and aggregation are the body's natural primary haemostatic response to vascular injury, followed by secondary haemostatic events of coagulation, clot formation, gradual clot retraction and healing 1›2. In the event of atherosclerosis-associated plaque erosion, rupture, and/or interventional procedure-associated endothelial disruption/denudation, the haemostatic responses to the vascular injury can become dysregulated, leading to excessive thrombus formation and subsequent clotting, luminal occlusion, ischemia, tissue morbidity and mortality. The timely diagnosis of these events, proper restoration of blood flow, and the prevention of event recurrence are critical for tissue survival and vascular function retrieval. Consequently, extensive therapeutic, diagnostic, endovascular and surgical procedures are undertaken in the analysis and treatment of thrombo-occlusive events in peripheral, cardiac and cerebral arteries. Often, medical

*Corresponding author: Case Western Reserve University, Department of Biomedical Engineering, 10900 Euclid Avenue, Cleveland, OH 44106.

facilities have limited options to implement complicated endovascular and surgical procedures. Hence therapeutic management of thrombo-occlusive events still remain the principal clinical option in the global perspective. The therapeutic management involves systemic (oral or trans-catheter) administration of anti-platelet, anti-coagulatory and fibrinolytic/thrombolytic agents. Such systemic administration often requires prolonged dosage to overcome the usually short half-life of the drugs and results in non-specific drug uptake, reduced therapeutic efficacy and systemic side-effects like hemorrhage. Intuitively, site-selective localization of the drugs can minimize non-specific uptake and systemic unwanted effects. This need for site-selectivity can be partly met by catheter-infused delivery of drugs proximal to the thrombotic sites or catheter-directed placement of drug-eluting stents following angioplastic procedures. However, such procedures are invasive, expensive, and depending on patient condition, may require additional procedural or post-procedural prolonged therapeutic management and care to prevent occlusion recurrence (e.g. in restenosis). Other surgical procedures like atherectomy and bypass grafting can also result in sub-acute levels of vascular injury leading to subsequent amplification into occlusion recurrence, thereby requiring prolonged post-procedural therapeutic regimen. In consideration of such pros and cons of current therapeutic management of vascular diseases, we have hypothesized that an injectable nanoparticle encapsulating a suitable drug, protecting it in circulation from plasma clearance and non-specific uptake, and delivering it preferentially to a vascular injury site, can become a stand-alone or adjunctive way of minimally invasive yet site-selective vascular drug delivery. To this end, we are developing lipid-based nanoscale unilamellar vesicles (liposomes), that are surface-decorated with peptide ligands having specificity and high affinity to integrin GPIIb-IIIa, a cell-surface receptor stimulated into a ligand-binding conformation uniquely on activated platelets.

The choice of activated platelets as the cellular target for our nanoparticles is based on the rationale that active platelets play a major role in the development and progression of all pathologic events in vascular disease. The various cellular interactions of platelets relevant to vascular pathology are shown schematically in Figure 1. On inflamed/dysfunctional endothelium (EC) of injured/diseased blood vessel, the endothelial surface expression of von Willebrand factor (vWf) and P-selectin promotes platelet tethering and rolling via interaction with platelet integrin GPIb/IX/V and platelet P-selectin glycoprotein ligand-1 (PSGL-1), respectively 3‚4‚5. Activated platelets can further secure themselves at the injury site by interaction of active platelet integrins GPIIb-IIIa and $\alpha_5\beta_1$ with subendothelial fibronectin, and platelet integrin $\alpha_2\beta_1$ with subendothelial collagen 6‚7. In pro-inflammatory environment associated with vascular diseases like atherosclerosis, endothelium- and subendothelium-adhered platelets also promote adhesion of inflammatory cells like monocytes via interaction between platelet P-selectin and monocyte PSGL-18. Platelets also produce chemokines and cytokines like platelet derived growth factor (PDGF) and transforming growth factor β (TGF-β) that promote cellular migration and activity in atherosclerosis-associated inflammation 9. Secretion of certain matrix metalloproteases (MMPs) from platelets contribute to matrix degradation and reorganization during atherosclerotic progression. Finally, in thrombo-occlusive events associated with acute vascular injury (e.g. plaque rupture), activated platelets undergo fibrinogen (Fg)-mediated interplatelet bridging via specific interaction between Fg and platelet surface integrin GPIIb-IIIa, to form the platelet plug 10. Further coagulatory events promoted by factors co-localized on the activated platelet membranes result in the occlusive clot11. Based upon such mechanistic criteria, *nanoparticles targeting to activated platelets* can potentially provide a way for site-selective diagnostic and therapeutic actions in a variety of vascular disease situations.

The bioengineering design of our platelet-targeted liposomes is based on the Arginine-Glycine-Aspartic Acid (RGD) sequence-mediated interaction of native ligands (e.g.

fibrinogen, fibronectin) to active platelet GPIIb-IIIa that results in platelet-matrix adhesions and platelet-platelet bridging. Because of this specific ligand-receptor interaction, several RGD-based small molecular weight peptides have been developed as anti-GPIIb-IIIa (hence anti-platelet) agents 12¯15, whose main function is to block the GPIIb-IIIa integrins and thereby prevent platelet adhesion and aggregation. Following this rationale, we have developed liposomes whose surfaces are decorated with multiple copies of GPIIb-IIIa-specific RGD ligands such that they can specifically bind activated platelets 16¯18. Here, we report our recent microscopy studies of active platelet binding by liposomes surface-decorated with a high affinity cyclic RGD peptide. To assess platelet-binding ability, we incorporated a lipophilic fluorophore within the liposomes and incubated test (surface modified with specific targeting cyclic RGD peptide) and control (surface modified with non-specific RGE peptide) liposomes with activated human platelets, followed by analysis of the incubated cells with fluorescence microscopy and phase contrast microscopy. The resolution limits of fluorescence microscopy resolution makes it difficult to visualize nanoscale liposomes on activated platelets. To obtain this complimentary evidence, we developed the same liposomes where instead of a fluorophore, we incorporated Nanogold® in the liposomal membrane, and analyzed the liposome-incubated platelets by high resolution scanning electron microscopy (SEM). After confirming platelet-targeting in vitro by fluorescence, phase contrast and SEM techniques, the liposomes were tested in vivo in rats in an acute restenosis model created by catheter-induced endothelial denudation of carotid artery. The liposome-exposed injured vessels were excised from euthanized animals and were imaged ex vivo by fluorescence microscopy and SEM. The in vitro and ex vivo imaging results, reported here, provided promising evidence to support our nanoparticle design for targeted vascular delivery.

2. Materials and Methods

Reagents

Amino acid derivatives, activator (1-hydroxy-1-azabenzotriazoleuronium, HATU), and synthesis resin were purchased from Anaspec, Inc. An activated, purified synthetic polyethylene oxide (PEO) derivative of distearoylphosphatidylethanolamine containing a terminal N-hydroxysuccinimide activated carboxyester (DSPE-PEG-COO-NHS) was purchased from NOF America Corporation. The PEO component had a reported average molecular weight of 2000. Cholesterol, distearoylphosphatidyl choline (DSPC), 1,2-distearoyl-*sn*-glycero-3-phosphoethanolamine-N-[methoxy(polyethylene glycol)-2000] (abbreviated as DSPE-PEO_{2000}) and 1-palmitoyl-2-[12-[(7-nitro-2-1,3-benzodiazol-4-yl)]amino]dodecanoyl]-*sn*-glycero-3-phosphocholine (abbreviated as PDPC-NBD) were purchased from Avanti Polar Lipids. For the synthesis of nanogold labeled liposomes, dipalmitoyl phophatidyl ethanolamine Nanogold® (abbreviated as DPPE-Nanogold®) was purchased from Nanoprobes (Yaphank, NY) and refrigerated at 2–8 ° C. Bovine serum albumin (BSA), human collagen III, phosphate buffered saline (PBS), HPLC grade solvents and sodium citrate were obtained from Sigma Aldrich (St. Louis, MO). For rat platelet staining, FITC-conjugated mouse anti-rat CD42d (staining rat platelet glycoprotein V) monoclonal antibody was obtained from BD Biosciences. For in vitro platelet studies, human blood was obtained from aspirin-refraining consenting donors within the department of Biomedical Engineering at Case Western Reserve University.

Synthesis of peptide ligands, lipid-peptide conjugates and peptide-decorated liposomes

The cyclic RGD- peptide, namely, CNP***RGD***Y(-OEt)RC (designated as c-RGD, with terminal Cysteines cyclized), and a negative control peptide GSSSG***RGE***SPA (designated as RGE) were synthesized by solid-phase peptide synthesis using standard 9-fluoromethoxycarbonyl (Fmoc) chemistry 19. The rationale for choosing this particular

cyclic RGD-peptide sequence is based on IC_{50} values of cyclic peptides in GPIIb-IIIa binding assays reported in literature 12. The details of the peptide synthesis and the subsequent carbodiimide-mediated conjugation of amine-terminated peptide to N-hydroxysuccimimide (NHS)-activated carboxyl terminal of DSPE-PEG-COOH, followed by cleavage of this lipid-peptide conjugate from the resin, purification (by HPLC and dialysis) and characterization (by MALDI-TOF mass spectrometry), and subsequent formulation into liposomes using reverse phase evaporation and extrusion methods, have been described elsewhere18. In the liposome formulations, the concentration of test or control peptide-lipid conjugate was kept as 5 mol% of total lipid. The rest of the formulation consisted of 50 mol % DSPC, 44 mol% cholesterol, and, 1 mol% PDPC-NBD or DPPE-Nanogold. Liposomes surface-decorated with cyclic RGD peptide will be denoted as cRGD-liposomes and those decorated with RGE peptide will be denoted as RGE-liposomes henceforth. Dynamic light scattering (DLS) studies with a Brookhaven Model 90 Plus Particle Size Analyzer showed the average liposome size to be around 150 nm for all batches. Figure 2 shows a schematic of liposome preparation and representative DLS data for liposomes before and after extrusion.

Fluorescence and phase contrast microscopy studies and flow cytometry studies in vitro

Collagen-coated glass coverslips bearing monolayer of human platelets, activated by agonist ADP, were prepared as described elsewhere 17. Adhesion of activated platelet monolayer on coverslips was confirmed by staining representative coverslips with fluorescein isothiocyanate (FITC)-tagged mouse anti-human CD41a monoclonal antibody that stains platelet GPIIb-IIIa, and observing the fluorescence ($\lambda_{emission}$ ~ 525 nm, green fluorescence) using a Nikon Diaphot inverted microscope containing a filter cube with a 450–490 nm excitation filter, a 510 dichroic mirror and a 520–560 nm bandpass filter. After confirming presence of platelets, similar platelet-adhered coverslips were incubated with test cRGD-liposomes or control RGE- liposomes (8 μl with 25 μM total lipid per coverslip) containing PDPC-NBD as the fluorescent label. The liposome incubation was done in presence of 5 mM $CaCl_2$ solution since the interaction of RGD to active platelet GPIIb-IIIa is facilitated by Ca^{++} ions 20. The incubation was maintained for 1 hr in the dark. Afterwards the coverslips were gently washed with PBS, mounted on glass slides and imaged by the fluorescence microscope using the same filter parameters as that for FITC fluorescence. Parallel phase contrast image of the same field of view was obtained on the same microscope, by shutting off the fluorescence laser, turning on the phase contrast light source and changing the objective from fluorescence to a phase contrast one, at same magnification.

To establish that the specific binding of cRGD-liposomes is predominantly to activated platelets compared to quiescent platelets, we performed flow cytometry assays similar to that described in previous publications from our group16–18. Briefly, NBD-labeled cRGD-liposomes were incubated with aliquots of freshly drawn human whole blood with or without the addition of agonist ADP. We have previously shown17 by flow cytometric analysis of GPIIb-IIIa and P-selectin co-expression on the platelet surface, that freshly drawn human blood has about 25% platelet population in activated state due to procedural effects (blood draw, contact with syringe, contact with storage tube etc.). Upon addition of agonist (ADP or TRAP), this activation level increases to about 98%. NBD-labeled cRGD-liposomes were incubated at a concentration of 500 μM total lipid with 10 μl of human whole blood aliquot without pre-incubation or with pre-incubation of ADP. Following 30 min of liposome incubation, the aliquots were analyzed in a Becton-Dickinson FACScan flow cytometer for NBD fluorescence. All aliquots were measured in triplicate and approximately 15000 counts were recorded per aliquot. Aliquots without any liposome incubation was used as ‘unlabeled’ controls. The NBD fluorescence intensity from aliquots without liposome incubation, aliquots with liposome incubation but without ADP pre-

incubation, and aliquots with liposome incubation after ADP pre-incubation, were recorded as histograms and the plots were overlaid for comparison.

SEM Studies in vitro

Platelets were adhered from suspension onto collagen III-coated coverslips in presence of ADP as described previously. Presence of activated platelets adhered onto the collagen-coated coverslips were first confirmed by SEM to obtain results complimentary to the fluorescence studies. For this, the platelet-incubated coverslips were fixed in 2.5 % glutaraldehyde for 2 hours at 4° C, washed with PBS, dehydrated with graded series of ethanol solution (10, 30, 50, 70, 90, 95, and 100 %) and critical point dried in liquid CO_2. The SEM imaging was done by attaching the coverslips to sample stubs and sputter coating with platinum followed by observation with a Hitachi S-4500 field emission scope. After confirmation of the presence of activated adhered platelets, similar samples were incubated with Nanogold-incorporated test (cRGD) and control (RGE) liposomes for 1 hour at room temperature, in presence of $CaCl_2$. Liposome-incubated coverslips were again washed with PBS to remove liposome suspension, fixed in 2.5 % glutaraldehyde for 2 hours at 4° C, re-washed with PBS, dehydrated with graded series of ethanol solution, critical point dried in liquid CO_2 and analyzed with SEM using same instrument as described above. The microscope was operated in both secondary and back-scatter electron detection modes with an accelerating voltage of 5kV. All images were saved directly with a digital image acquisition system (Quartz PCI).

Ex vivo microscopy studies on platelet-targeting of liposomes in a rat carotid injury model

The catheter-induced acute injury model in rat carotid has been described elsewhere 18. This procedure of carotid injury has been utilized in several studies regarding role of platelets and other cells and biomolecules in regulating restenotic and intimal events 21⁻23. Following injury, the right common carotid and the descending aorta were ligated. The blood flow was reestablished (repurfusion) to allow flow of blood only through the injured left carotid vessel. The blood flow was resumed for 1hr or 2hrs to allow activation, adhesion and aggregation of platelets at the injury site due to an acute thrombotic/restenotic environment. Four animals, two immediately after injury and two after 1 hr reperfusion, were sacrificed and the injured vessel sections were excised and washed gently in PBS. Uninjured carotid sections were also excised from the already sacrificed animals for image analysis and comparison purposes. All sections were cut open longitudinally to expose the injured surface. One uninjured section and one 1 hr-repurfused injured section were subjected to incubation with FITC-tagged mouse anti-rat CD42d monoclonal antibody (emission ~ 525 nm, green fluorescence) which stains for rat platelet glycoprotein GPV 24. Following incubation for 1 hr in the dark, the sections were fixed with 4 % paraformaldehyde (PFA), washed gently with PBS, mounted on glass slides with luminal surface exposed and imaged with epifluorescence microscope using the same filter and objective specifications as used for the in vitro studies. The other uninjured, injured and repurfused sections were fixed in 3.0% glutaraldehyde in PBS at 4°C overnight, washed with 50 mM glycine in PBS to remove excess aldehydes, and then washed with distilled water. Following this, the sections were dehydrated in a graded series of ethanol solutions as described previously for the in vitro SEM samples, critical point dried in liquid CO_2, mounted on sample stubs, sputter coated with platinum and observed with the previously mentioned EM instrument in both secondary and back-scatter modes with an accelerating voltage of 5kV. The fluorescence and the SEM analyses of the injured carotid sections vs uninjured sections were done to confirm the presence of activated adhered platelets in the acute injury environment of our model. Following confirmation, similar animals were exposed to fluorescently labeled or Nanogold-labeled test and control liposomes. At the end of the 1 hr or 2 hr blood reperfusion period through the injured vessel, NBD-labeled or Nanogold-labeled cRGD- and RGE-

liposomes were injected into the left ventricle of the rat heart to allow the flow of liposomes along with the blood pumped into the injured carotid. For the ex vivo imaging studies, statistical power calculations were based on the area of coverage of the injured luminal surface by fluorescently labeled liposomes, as obtained by morphometric analysis (by Metamorph and Image J) of digital images. General background levels appear to be ~ 5% of the area. Our power calculation was based on seeing a 100% increase (to 10% coverage) with 80% power. Based on these parameters our calculation suggested a sample size of ~4 animals per liposome formulation. For NBD-labeled test and control liposomes, four animals were used per formulation. For Nanogold-labeled test and control liposomes, two animals were used per formulation, since this analysis was more qualitative. After liposome injection, the reperfusion flow was maintained for 15 minutes, at the end of which the rats were sacrificed and the injured vessels were excised, washed gently by PBS and prepared for fluorescence or SEM imaging.

For fluorescence imaging, the sections were fixed in 4% PFA, re-washed with PBS, sliced open longitudinally, and the luminal side was imaged with the previously described inverted epifluorescence microscope for NBD fluorescence. At least eight images were obtained per section. For SEM imaging, the excised tissue sections were sliced open longitudinally, fixed in 3.0% glutaraldehyde, washed with 50 mM glycine and then in distilled water. To facilitate imaging of Nanogold-labeled liposomes within the complex morphology injured tissue, gold autometallography was used to enhance the size of Nanogold. This was achieved using a commercially available autometallography kit “Goldenhance-EM” (Nanoprobes) and following the supplier instructions. The tissues were immersed in the enhancement solution for 15 minutes, which according to the supplier, can increase the Nanogold size to ~ 20 nm. Control tissue sections, without Nanogold-labeled liposome exposure but with exposure to the Goldenhance solution were prepared to check for non-specific background enhancement in SEM. After enhancement, all sections were washed with distilled water, dehydrated in a graded series of ethanol solutions, critical point dried in liquid CO_2 and analyzed with SEM. At least eight images were obtained per tissue section.

Data Analysis

For in vitro and ex vivo fluorescence images of liposome-incubated platelets, surface-averaged fluorescence intensity was measured using Metamorph® software. For analysis and comparison purposes, the camera parameters were kept constant for all in vitro studies. For the ex vivo studies, the camera conditions were different from the in vitro conditions, but were kept constant for all ex vivo images. Statistical analysis, where applicable, was performed in Microsoft Excel using a two tailed, unpaired student’s t test (assuming unequal variance) to compare the difference in fluorescence intensity. Significance was considered as $p < 0.05$. All data was noted as mean ± SD. For in vitro and ex vivo SEM studies, the image acquisition parameters were kept constant and the results were compared qualitatively.

3. Results

In Vitro Fluorescence Microscopy Studies and Flow Cytometry Studies on Liposome-incubated Human Platelets

Figure 3 shows representative microscopy images for coverslip-adhered ADP-activated human platelets incubated with (3A) RGE-liposomes and (3B) cRGD-liposomes, in presence of Ca^{++}. Figures 3A and 3B are representative of images captured through 10X objective. As evident from the images, qualitatively, the binding of cRGD-liposomes to the activated platelets was considerably higher than that for RGE-liposomes. Figure 3E shows the mean fluorescence intensity data for samples incubated with RGE-liposomes and cRGD-

liposomes. Statistical analysis of average fluorescence intensity of images from multiple batches of experiments showed that fluorescence intensity of NBD-labeled cRGD-liposome incubated platelet-adhered coverslips were significantly higher ($p < 0.01$) compared to that from RGE-liposome incubated platelet-adhered coverslips, indicating enhanced platelet-binding of the cRGD-liposomes. The cRGD-liposome incubated samples were observed further at higher magnification with 60X oil-immersion objective. Figures 3C and 3D show representative fluorescence and phase contrast images respectively, with 60X objectives, of the same field of view for a c-RGD-liposome incubated platelet-adhered coverslip. The one-to-one correspondence of the fluorescence spots with activated platelets can be observed from 3C and 3D. Representative NBD fluorescence histograms from flow cytometry analyses are shown in Figure 3F; liposome incubation with predominantly inactive platelet population (no ADP pre-incubation) resulted in NBD intensity close to that of baseline 'unlabeled' while that with ADP-activated platelets increased NBD fluorescence from the gated platelet population by almost two orders of magnitude. Such analyses further confirmed that the binding of the cRGD-liposomes were specifically enhanced to active platelets, and the non-specific platelet binding of cRGD-liposomes was minimal.

In vitro SEM studies on liposome-incubated human platelets

Figure 4 shows representative images from SEM studies of platelet-adhered coverslips incubated with Nanogold-labeled cRGD- and RGE-liposomes. Figure 4A and the enlarged image in Figure 4B, are representative SEM images of the coverslip surface after the experimental procedure of incubating a suspension of human platelets on the collagen-coated glass coverslips in presence of agonist ADP. As evident from the images, the procedure resulted in formation of an adhered monolayer of highly activated platelets. The highly activated state is emphasized by the 'spread' morphology, highly folded membrane appearance and the numerous pseudopodal extensions of the platelet membrane as seen in Figures 4A and 4B. Similar coverslip-adhered platelets were incubated with Nanogold-labeled cRGD- and RGE-liposomes and imaged with SEM. Due to the highly convoluted appearance of the activated platelet membrane, it is difficult to conclusively distinguish between a membrane fold and a vesicular liposome attached to the membrane from secondary electron images. Hence, backscatter images were also obtained for the same platelets with the rationale that the gold-labeled nanoparticles, if bound to the platelets, will produce enhanced backscatter and hence will enable higher resolution visualization of the nanoparticles, compared to the normal backscatter from platelet membrane folds. Figures 4C1 and 4C2 show respectively the secondary electron mode and the backscatter mode images of a representative platelet on coverslips incubated with RGE-liposomes. While the secondary electron mode image shows numerous folds and bulges on the membrane that apparently may look like liposomal particles, the backscatter image of the same platelet shows only minimal contrast-enhancement on the platelet membrane, thereby suggesting that the folds and bulges seen in the secondary electron mode image are mainly convolutions and vesicular protrusions of the platelet membrane itself (e.g. vesiculation into microparticles), with maybe minimal non-specific binding of gold-labeled liposomes by possible lipid exchange. Figures 4D1 and 4D2 show respectively the secondary electron mode and the backscatter mode images of a representative platelet on coverslips incubated with cRGD-liposomes. Once again the secondary electron mode image shows folds, bulges and vesicular protrusions on the platelet membrane similar to the RGE-liposome incubated samples. However, backscatter image of the same field shows significant bright contrast of the platelet membrane compared to the representative sample from the RGE-liposome incubated batch. Also, multiple highly contrast-enhanced vesicular structures (highlighted by arrowheads) adhered onto the platelet membrane and the platelet pseudopodal extensions are visible on the representative image from the cRGD-liposome incubated batch. From the scale bar, the size of these structures are around 100–200 nm and hence most possibly they

are Nanogold-labeled liposomes. These results suggest enhanced binding and fusion of gold-labeled cRGD-liposomes with the platelet membrane. Considering these results to be complimentary to the results obtained from fluorescence microscopy studies, it can be concluded that the cRGD-liposomes have enhanced binding, specifically to activated platelets, and hence can be promising towards platelet-directed site-selective vascular delivery.

Ex vivo microscopy studies of liposome-platelet interactions in rat carotid injury model

Figure 5 shows the schematic of experimental procedure (5A), a collection of representative SEM and fluorescent images of the carotid wall before (5B and 5D) and after injury (right after injury, 4E, and, after 1 hr repurfusion, 5C and 5F). Figure 5 also shows representative fluorescent images of the injured carotid exposed to NBD-labeled RGE-liposomes following 1 hr (5H) and 2 hr (5J) repurfusion, and the injured carotid exposed to NBD-labeled cRGD-liposomes following 1 hr (5I) and 2 hr (5K) repurfusion, along with the statistical analysis of fluorescent images from all batches of this study (5L). As evident from 5B, the uninjured rat tissue itself has autofluorescence associated with it. The SEM image of the uninjured tissue (5D) shows uniform striated appearance given by luminal lining of cells, while upon catheter-induced injury, acute disruption of the luminal wall is visible (5E). After perfusion of blood through the injury site for 1 hr, staining with FITC-tagged anti-rat CD42d and imaging with epifluorescence microscope revealed numerous adhered platelets on the injured luminal wall (5C). This data was complimented by SEM analyses of similar samples, where numerous adhered platelets were visible on the injured wall (5F) and upon further magnification, platelets were found to be arrested in and adhered to fibrin mesh (5G), signifying an acute thrombotic/restenotic environment. The 15-minute exposure of the injured carotid to NBD-labeled RGE-liposomes (in flowing blood) after repurfusion for 1 hr (5H) and 2 hrs (5J) showed only minimal staining of platelets over the background autofluorescence. The same for NBD-labeled c-RGD-liposomes showed significant platelet staining over background autofluorescence for both 1 hr (5I) and 2 hr (5K) repurfusion situations. Statistical analysis of average fluorescence intensity of images from multiple batches of experiments confirmed this observation (5L). As evident from the representative image 5K, fluorescence microscopy analysis of c-RGD-liposome exposed injured carotid after 2 hr perfusion period also showed indication of acute platelet aggregation and clotting (green fluorescent clumps in 5K).

Figure 6 shows representative secondary mode and backscatter mode SEM images of injured carotid wall exposed to Nanogold-labeled RGE-liposomes (6A1 and 6A2) and cRGD-liposomes (6B1 and 6B2). Secondary electron mode images for both RGE-liposome and cRGD-liposome exposed injured carotid wall looked very similar (6A1 and 6B1), revealing dense fibrin mesh and adhered/arrested platelets. However the backscatter mode images for cRGD-liposome exposed injury site (6B2) showed considerably bright contrast compared to RGE-liposome exposed injury site (6A2). This suggests enhanced binding of gold-labeled cRGD-liposomes to the injury site, most possibly, by design, to the activated platelets adhered and aggregated at the site. Because of the highly irregular three-dimensional dense morphology of the thrombotic environment, the dynamic flow environment of the experimental protocol, and the complex ex vivo sample preparation procedures, the intact vessel integrity of platelet-adhered liposomes was probably not maintained in these in vivo experiments, as it was maintained for the static incubation experiments in vitro. Nonetheless, the enhanced brightness of cRGD-liposome exposed tissue suggested enhanced site-specific liposome binding, complimentary to the fluorescence microscopy data of Figure 5.

4. Discussion

Nanoparticle-based delivery systems that can actively target disease-associated cells based upon molecular interaction with cell-surface receptors provide enhanced warrantee of cell-selective/site-selective localization of nanoparticle-encapsulated bioactive agents. For such active targeting to work, the prerequisites are, firstly, for the nanoparticles to be able to reach the cells, and secondly, to be able to out-compete native ligands that bind the same cell-surface receptors. For certain deep tissue disease situations, like in cancer, reaching the tumor cell is often contingent upon the nanoparticles extravasating and accumulating through leaky vasculature in the vicinity of the tumor mass. This is a passive targeting process commonly known as enhanced permeation and retention. Additional cell-binding properties based upon specific ligand-receptor interactions can then provide additional active targeting properties. This concept has been researched extensively using antibody-modified and peptide-modified nanoparticles for tumor-selective delivery 25. Passive targeting for cells in the vascular compartment is less relevant, since a population of nanoparticles can always reach the cells via blood flow. Hence for such situations, ‘active targeting’ becomes more important to ensure that the nanoparticles can bind to the target cells strongly under dynamic blood flow conditions. To ensure strong active binding, it is necessary to identify target cellular or biomolecular epitopes that are present in high quantity but uniquely in a disease environment. Also, it is necessary to identify nanoparticle-modifying ligands that will maintain high enough affinity to the target epitope to be able to out-compete native ligands. Such mechanistic considerations have guided our design of cyclic RGD-modified liposomal nanoparticles that can actively target and bind stimulated GPIIb-IIIa integrin receptors only on activated platelets. The choice of liposomes as the ‘platform’ nanoparticles is because of their ability to encapsulate both hydrophobic and hydrophilic agent, their biocompatibility and the possibility to fuse with cell membrane to facilitate active delivery once they bind the cell-surface receptor. Our results reported here provide groundwork to extend the studies into actual therapeutic/diagnostic formulations within the platelet-targeted liposomes for imaging and drug response analysis.

The in vitro fluorescence microscopy studies, complimented by flow cytometry studies, suggest extensive binding of cRGD-liposomes to activated platelets, while the in vitro SEM studies reveal only a few representative liposomes adhered onto platelets. It is to be noted that the number of liposomes ‘observed’ in the SEM studies do not necessarily reflect the extent of liposomes that actually ‘bind’ the activated platelets. It is possible for liposomes to fuse with platelet membrane after binding 26, in which case intact vesicle membrane integrity for liposomes will not be preserved and hence will not be visible by SEM. Also, the rigorous SEM sample preparation procedure may result in membrane collapse of majority of platelet-adhered liposomes. Hence the ‘observed’ liposomal structures in the SEM analysis represent only a small percentage of ‘bound’ liposomes whose membrane integrity was fortunately preserved through the whole process. The enhanced platelet-binding of cRGD-liposomes is evidenced more by the bright contrast enhancement of the platelet membrane as a whole. This effect is more pronounced in the ex vivo SEM images of the injured rat carotid samples.

It is also to be noted that for the carotid injury model, the liposomes were injected relatively proximal to the injury site and the ligation of different vessels ensured flow of these liposomes (in blood) predominantly to the injury site. In an actual physiological environment, the liposomes are envisioned to be administered via I.V.-injection and should be able to stay in circulation long enough to recognize and bind at vascular sites exhibiting platelet hyperactivity and aggregation. Hence, future studies would be directed at surface-modification of the platelet-targeted liposomes with high degree of PEGylation to ensure enhanced circulation time and subsequent studies in animal vascular injury models with

I.V.-administration. Nonetheless, our current studies provide convincing in vivo evidence of enhanced platelet-binding by cRGD-liposomes in an acute vascular injury environment.

Acknowledgments

The authors acknowledge the help from Dr. Zhongmin Zhou and Dr. Marc S Penn at The Cleveland Clinic Foundation in conducting the restenosis model studies. The authors also acknowledge the help of John Sears in the Department of Materials Science and Engineering at Case Western Reserve University for helping with the SEM studies. Facilities for in vitro studies were provided by Center for Cardiovascular Biomaterials at Case Western Reserve University. The research was partly supported by NIH (research grant HL-70263).

References

1. Michelson, AD. Platelets. Academic Press; 2002.
2. Munker, R.; Hiller, E.; Glass, J.; Paquette, R. Biology and Clinical Management. Totowa, NJ: Humana; 2007. Modern Hematology.
3. Gawaz M, Langer H, May AE. Platelets in inflammation and atherogenesis. J Clin Invest. 2005; 115:3378–3384. [PubMed: 16322783]
4. Ruggeri ZM. Platelets in atherothrombosis. Nature Medicine. 2002; 8:1227–1234.
5. Frenette PS, Denis CV, Weiss L, Jurk K, Subbarao S, Kehrel B, Hartwig JH, Vestweber D, Wagner DD. P-selectin Glycoprotein Ligand 1 (PSGL-1) is expressed on platelets and can mediate platelet-endothelial interactions in vivo. J Exp Med. 2000; 191:1413–1422. [PubMed: 10770806]
6. Bombeli T, Schwartz BR, Harlan JM. Adhesion of activated platelets to endothelial cells: Evidence of GPIIbIIIa-dependant bridging mechanism and novel roles of endothelial intercellular adhesion molecule 1 (ICAM-1), $\alpha_V\beta_3$ integrin and GPIbα. J Exp Med. 1998; 187:329–339. [PubMed: 9449713]
7. Verheul HMW, Jorna AS, Hoekman K, Broxterman HJ, Gebbink MFBG, Pinedo HM. Vascular endothelial growth factor-stimulated endothelial cells promote adhesion and activation of platelets. Blood. 2000; 96:4216–4221. [PubMed: 11110694]
8. Lusis AJ. Atherosclerosis. Nature. 2000; 407:233–241. [PubMed: 11001066]
9. von Hundelshausen P, Weber KSC, Huo Y, Proudfoot AEI, Nelson PJ, Ley K, Weber C. RANTES deposition by platelets triggers monocyte arrest on inflamed and atherosclerotic endothelium. Circulation. 2001; 103:1772–1777. [PubMed: 11282909]
10. Plow EF, D'Souza SE, Ginsberg MH. Ligand binding to GPIIb-IIIa: a status report. Semin Thromb Hemost. 1992; 18:324–332. [PubMed: 1455250]
11. Plow EF, Pierschbacher M, Ruoslahti E, Marguerie G, Ginsberg MH. Arginyl-glycyl-aspartic acid sequences and fibrinogen binding to platelets. Blood. 1987; 70:110–115. [PubMed: 3036276]
12. Cheng S, Craig WS, Mullen D, Tschopp JF, Dixon D, Piersbacher MD. Design and synthesis of novel cyclic RGD-containing peptides as highly potent and selective integrin $\alpha_{IIb}\beta_3$ antagonists. J Med Chem. 1994; 37:1–8. [PubMed: 7507165]
13. Coutre S, Leung L. Novel antithrombotic therapeutics targeted against platelet glycoprotein IIb/IIIa. Ann Rev Med. 1995; 46:257–265. [PubMed: 7598462]
14. O'Shea JC, Hafley GE, Greenberg S, Hasselblad V, Lorenz TJ, Kitt MM, Strony J, Tcheng JE. Platelet glycoprotein IIb/IIIa blockade with eptifibatide in coronary stent intervention. The ESPRIT trial: a randomized control trial. J Am Med Assoc. 2001; 285:2468–2473.
15. Sow MA, Molla A, Lamaty F, Lazaro R. Synthesis of RGD amphiphilic cyclic peptide as fibrinogen or fibronectin antagonist. Letters in Peptide Science. 1997; 4:455–461.
16. Lestini BJ, Sagnella SM, Xu Z, Shive MS, Richter NJ, Jayaseharan J, Case AJ, Kottke-Marchant K, Anderson JM, Marchant RE. Surface modification of liposomes for selective targeting in cardiovascular drug delivery. J control Rel. 2002; 78:235–247.
17. Sen Gupta A, Huang G, Lestini BJ, Sagnella S, Kottke-Marchant K, Marchant RE. RGD-modified liposomes targeted to activated platelets as a potential vascular drug delivery system. Thromb Haem. 2005; 93:106–114.

18. Huang G, Zhou Z, Srinivasan R, Penn MS, Kotke-Marchant K, Marchant RE, Sen Gupta A. Affinity manipulation of surface-conjugated RGD peptide to modulate binding of liposomes to activated platelets. Biomaterials. 2008; 29:1676–1685. [PubMed: 18192005]
19. Fields GB, Noble RL. Solid phase peptide synthesis utilizing 9-fluorenylmethoxycarbonyl amino acids. Int J Pept Protein Res. 1990; 35:161–214. [PubMed: 2191922]
20. D'Souza SE, Haas TA, Piotrowicz RS, Byers-Ward V, McGrath DE, Soule HR, Cierniewski C, Plow EF, Smith JW. Ligand and cation binding are dual functions of a discrete segment of the integrin b3 subunit: cation displacement is involved in ligand binding. Cell. 1994; 79:659–667. [PubMed: 7525080]
21. Chandrasekar B, Tanguay J-F. Platelets and Restenosis. J Am Coll Cardiol. 2000; 35:555–562. [PubMed: 10716455]
22. Le Breton H, Plow EF, Topol EJ. Role of platelets in restenosis after percutaneous coronary revascularization. J Am Coll Cardiol. 1996; 28:1643–1651. [PubMed: 8962547]
23. Tsuruta W, Yamamoto T, Suzuki K, Yoshida F, Matsumura A. Simple new method for making a rat carotid artery post-angioplasty stenosis model. Neurol Med Chir. 2007; 47:525–529.
24. Sato N, Kiyokawa N, Takada K, Itagaki M, Saito M, Sekino T, Suzuki T, Taguschi T, Mimori K, Lanza F, Fujimoto J. Characterization of monoclonal antibodies against mouse and rat platelet glycoprotein V (CD42d). Hybridoma. 2000; 19:455–461. [PubMed: 11152397]
25. Amiji, M. Nanotechnology for cancer therapy. CRC Press; 2006.
26. Nishiya T, Sloan S. Interaction of RGD liposomes with platelets. Biochem Biophys Res Commun. 1996; 224:242–245. [PubMed: 8694820]

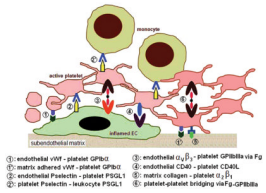

Figure 1.
Schematic diagram of possible cellular interactions of activated platelets at the site of a vascular injury/inflammation.

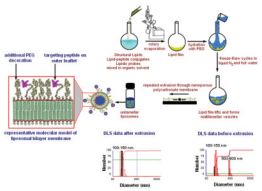

Figure 2.
Schematic diagram of the method of liposome preparation including a molecular model representation of the lipid bilayer membrane of the liposome, and the dynamic light scattering (DLS) analysis of liposome size distribution before and after extrusion through nanoporous membrane.

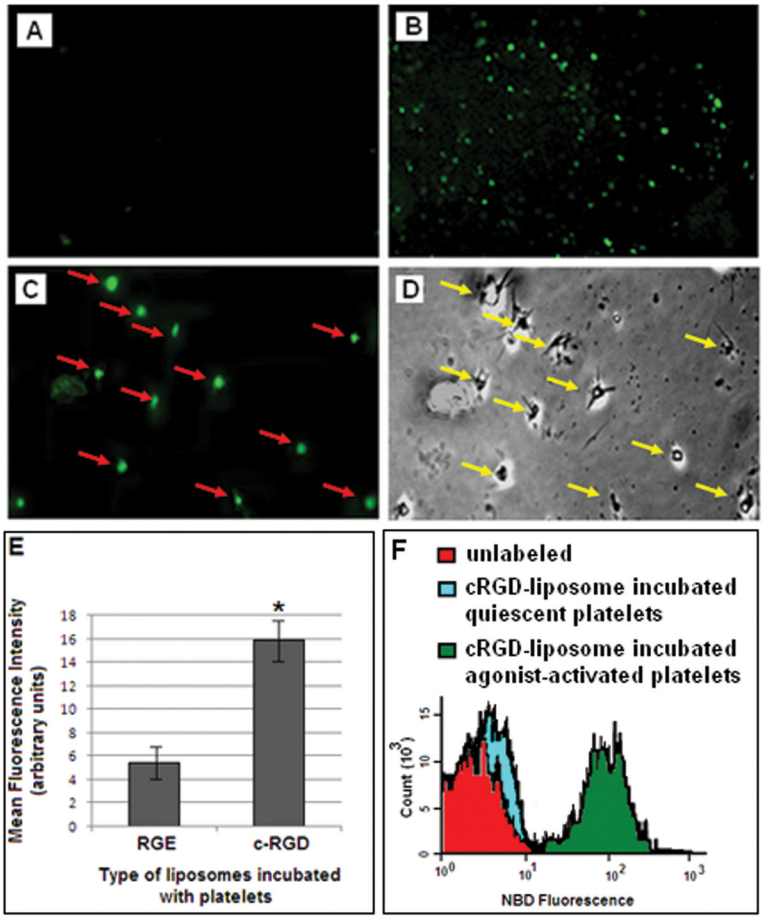

Figure 3.

Representative fluorescence and phase contrast microscopy images from in vitro studies of active platelet targeting by peptide-modified fluorescently labeled liposomes; (A) RGE-liposome-incubated sample showed minimal fluorescence, while (B) cRGD-liposome-incubated sample showed significantly enhanced fluorescence; parallel analysis of cRGD-liposome-incubated sample with (C) fluorescence and (D) phase contrast microscopy provided evidence for one-to-one correspondence of fluorescence spots with active platelets, thereby emphasizing that the liposome binding is platelet-specific; (E) represents the surface-averaged fluorescence intensity analysis of the RGE-liposome incubated and the cRGD-liposome incubated samples; (F) shows representative flow cytometry data of NBD fluorescence intensity histogram overlay for platelets without any liposome incubation, with liposome incubation but without ADP pre-incubation (predominantly inactive platelets) and with liposome incubation after ADP pre-incubation (predominantly active platelets), establishing that the NBD-labeled cRGD-liposomes have specific enhanced binding to *activated* platelets.

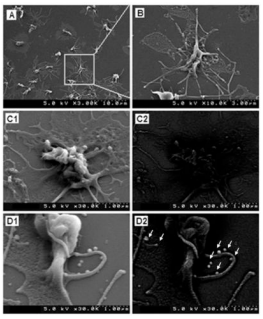

Figure 4.

Representative images from SEM studies of active platelet targeting by peptide-modified Nanogold-labeled liposomes; SEM analysis of collagen-coated coverslip exposed to human platelet suspension in presence of ADP showed (A) monolayer of adhered platelets which were in highly activated condition as evidenced by (B) highly folded membrane structure, ‘spread’ morphology and branched out pseudopods; SEM images in secondary electron mode of (C1) RGE-liposome-incubated platelet and (D1) cRGD-liposome-incubated platelet showed similar membrane morphology and vesicular structures, but corresponding images in backscatter mode showed (C2) minimal gold contrast enhancement on the membrane of RGE-liposome-incubated platelet, while (D2) significant contrast enhancement of the membrane of cRGD-liposome-incubated platelet; in addition, multiple bright spherical vesicular structures (arrowheads in D2) were visible on cRGD-liposome-incubated platelet, which are possibly intact liposomes adhered on the membrane and pseudopods.

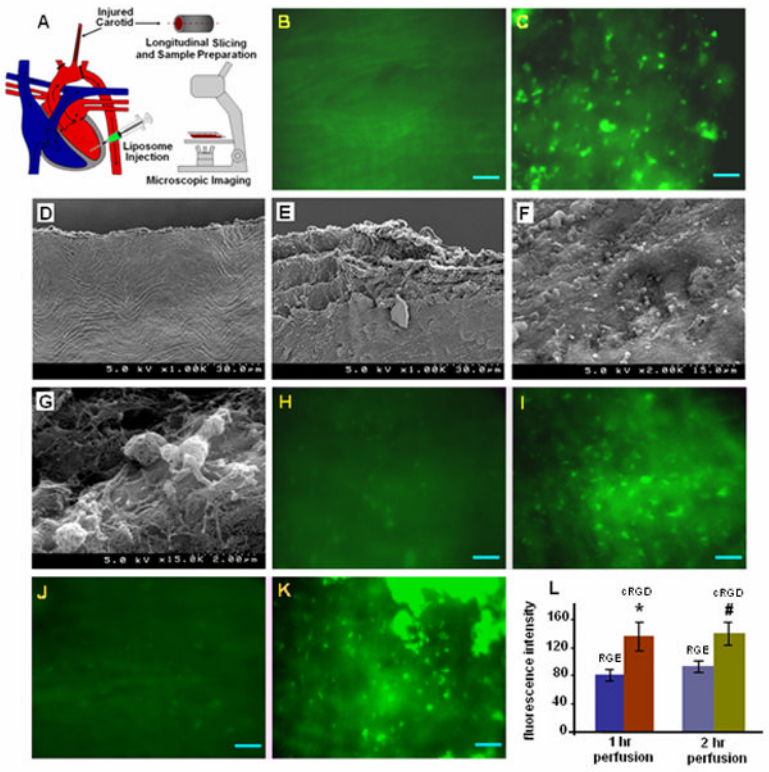

Figure 5.

Representative ex vivo images from studies of active platelet binding of peptide-modified fluorescently labeled liposomes in vivo in a rat carotid injury restenosis model; (A) shows the schematic of the in vivo model used in the study; (B) and (D) show representative fluorescence and SEM images of the carotid luminal surface without injury; (E) is an SEM image of the carotid luminal surface immediately after frictional injury with inflated balloon catheter, showing significant wall damage and endothelial denudation; after 1 hr of blood repurfusion through such injured carotid, SEM image of excised sections showed (F) numerous adhered platelets and upon magnification (G) arrested platelets in dense fibrin mesh were visible, signifying acute thrombotic environment; the presence of adhered platelets was confirmed by (C) fluorescence imaging after staining the injured section with FITC-tagged anti-rat CD42d (stains platelet GPV); introduction of fluorescently labeled RGE-liposomes in the injured section after (H) 1 hr and (J) 2 hr blood repurfusion showed only minimal staining of platelets; in contrast, introduction of fluorescently labeled cRGD-liposomes showed significant platelet staining in both (I) 1 hr and (K) 2 hr repurfusion situations; for 2 hr repurfusion sections, highly fluorescent clumps of aggregated platelets were also visible; (L) statistical analysis of fluorescence intensity from images of liposome-exposed carotid sections for several batches of animals, confirmed the enhanced binding of cRGD-liposomes at the injury site.

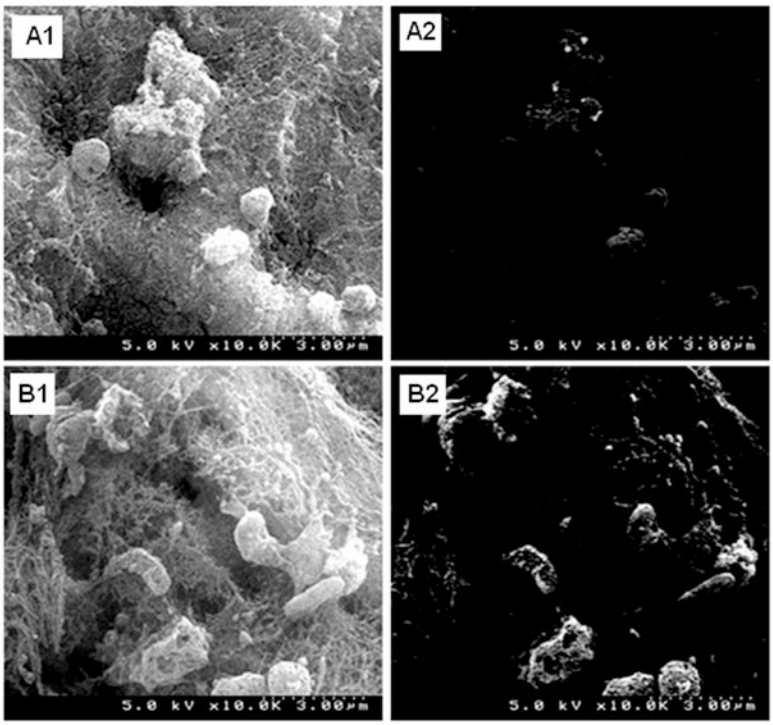

Figure 6.

Representative ex vivo SEM images from studies of active platelet targeting by peptide-modified Nanogold-labeled liposomes in vivo in a rat carotid injury restenosis model; the secondary electron mode images of both (A1) RGE-liposome-incubated and (B1) cRGD-liposome-incubated samples showed similar acute thrombotic environment with platelets arrested in dense fibrin mesh, but the corresponding backscatter image (A2) of RGE-liposome-incubated sample showed only minimal contrast enhancement while the backscatter image (B2) of cRGD-liposome-incubated sample showed substantial contrast enhancement of cellular structures arrested in the fibrin mesh, suggesting enhanced binding of Nanogold-labeled cRGD-liposomes to platelets.